Supramolecular Chemistry
Publication details, including instructions for authors and subscription information:
http://www.informaworld.com/smpp/title~content=t713649759

Clathrate Engineering of Piedfort Hosts. Crystal Structures and Molecular Modeling of the *para-mono-* and *meta*-di-methy1/*t*-buty1 Substituted Derivatives of 2,4,6-tris (alkylphenoxy)-1,3,5-triazine

László Fébián[a]; Petra Bombicz[a]; Mátyás Czugler[a]; Alajos Kálmán[a]; Edwin Weber[b]; Manfred Hecker[b]
[a] Institute of Chemistry, Chemical Research Center, Hungarian Academy of Sciences, Budapest, Hungary [b] Technische Universität Bergakademie Freiberg, Institut für Organische Chemie, Freiberg/Sachs., Germany

To cite this Article Fébián, László , Bombicz, Petra , Czugler, Mátyás , Kálmán, Alajos , Weber, Edwin and Hecker, Manfred(1999) 'Clathrate Engineering of Piedfort Hosts. Crystal Structures and Molecular Modeling of the *para-mono-* and *meta*-di-methy1/*t*-buty1 Substituted Derivatives of 2,4,6-tris (alkylphenoxy)-1,3,5-triazine', Supramolecular Chemistry, 11: 2, 151 — 167
To link to this Article: DOI: 10.1080/10610279908048726
URL: http://dx.doi.org/10.1080/10610279908048726

SUPRAMOLECULAR CHEMISTRY, Vol. 11, pp. 151–167
Reprints available directly from the publisher
Photocopying permitted by license only

Clathrate Engineering of Piedfort Hosts. Crystal Structures and Molecular Modeling of the *para-mono-* and *meta*-di-methyl/*t*-butyl Substituted Derivatives of 2,4,6-tris (alkylphenoxy)-1,3,5-triazine

LÁSZLÓ FÁBIÁN[a], PETRA BOMBICZ[a], MÁTYÁS CZUGLER[a,*], ALAJOS KÁLMÁN[a], EDWIN WEBER[b] and MANFRED HECKER[b]

[a] *Institute of Chemistry, Chemical Research Center, Hungarian Academy of Sciences, H-1525 Budapest, P.O. Box 17, Hungary;*
[b] *Technische Universität Bergakademie Freiberg, Institut für Organische Chemie, Leipziger Str. 29, D-09596 Freiberg/Sachs., Germany*

(Received 14 May 1999; In final form 21 May 1999)

X-ray crystal structure analyses of four related *2,4,6-tris-(alkylphenoxy)-1,3,5-triazine* host candidates were planned to clarify conditions of the *Piedfort pair* based inclusion formation. The *3,5-di-t-butyl-phenoxy* substituted compound yields inclusion and exhibits dimorphism as well. Contrasting the inclusion, no Piedfort pairing was observed in the dimorphs. Other *para-* and *meta-t*-butyl/methyl substituted molecules did not give clathrates. Homomolecular columns of polymeric Piedfort stacks were formed instead. The stacking distances between triazine rings in the polymeric columns vary smoothly with the size and position of the substituents. We conclude that bulky substituents must impede parallel to the expected direction of favorable Piedfort stacking to form inclusion supramolecules.

Keywords: Polymeric Piedfort complex, inclusion compounds, crystal structures, molecular modeling

INTRODUCTION

One of the basic tasks in supramolecular chemistry [1] is the rational design of host molecules [2]. This implies engineering of weak intermolecular interactions and using fine details of their balance. This is only recently put into practice in the form of crystal engineering [3,4]. In its most common form it requires the knowledge of some analogous structures so the task remains to be completed.

Recent efforts aimed at utilizing molecules with C_3 symmetry were both focusing on possible applications, *e.g.*, in octupolar non-linear optical materials design [4] and on synthetic and complexation aspects in general [5]. Such molecules attract considerable interest due to their inherent requirements to yield to trigonal stacks/nets of

*Corresponding author. Tel.: 36-1-325 7547, Fax: 36-1-325 7554, e-mail: czu@cric.chemres.hu

molecules in the form of, *e.g., Piedfort type associations* [6].

The Piedfort concept of host design [6] is based on an abstraction of the so called hexahosts idea [7]. It implies that a *sym-hexa*substituted benzene molecule is mimicked by a self-assembled dimer of *sym*-1,3,5-*tri*substituted six-membered aromatic rings [6] (Scheme 1). The hexahosts are often located on centers of inversion in the crystals. The two molecules of a Piedfort unit may also be related by this symmetry element [8]. According to the preferred geometry of $\pi-\pi$ interactions [9], the central rings have to be properly polarized to allow for such a close arrangement without a lateral offset. The contribution of these rather weak interactions to the overall stabilization of the crystal may or may not suffice to preserve the associates. Therefore this is a fairly non-trivial crystal engineering strategy since it implies the use of relatively labile supramolecular building blocks, the Piedfort pairs, to construct a macroscopic inclusion crystal.

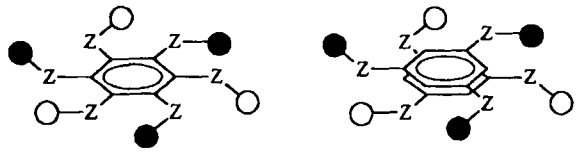

SCHEME 1

Crystal structures of several related 2,4,6-triaryloxy-1,3,5-triazines were reported recently [4]. It was established that these molecules form quasi-trigonal or trigonal networks. The role of *o*-hydrogen atoms on the aryloxy groups was emphasized in the formation of Piedfort units *via* CH···O and CH···N interactions. Inclusion formation was observed with 2,4,6-tris-(4-chlo-

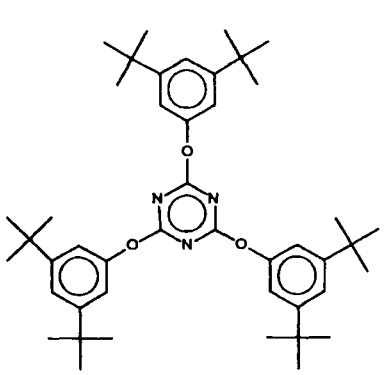

1

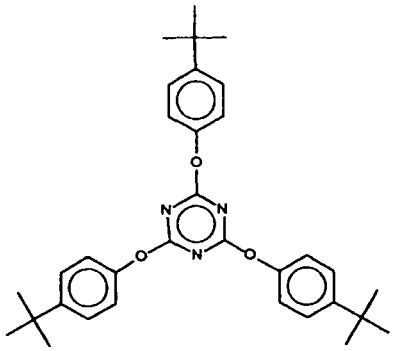

2

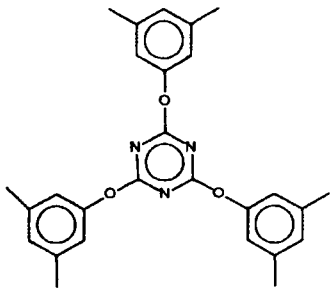

3

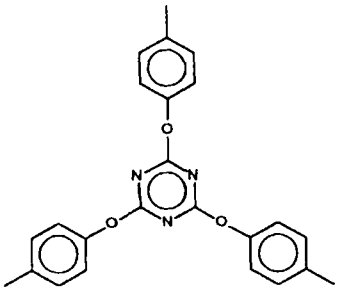

4

SCHEME 2

rophenoxy)-1,3,5-triazine and 2,4,6-tris-(4-bromophenoxy)-1,3,5-triazine. These molecules form large hexagonal cavities supported by trimeric X_3 (X = Cl, Br) supramolecular synthons [4a].

A plan was set to investigate crystal structures of the four related putative host molecules 2,4,6-*tris*-(3,5-*di-t-butylphenoxy*)-1,3,5-*triazine* (**1**), 2,4,6-*tris*-(4-*t-butylphenoxy*)-1,3,5-*triazine* (**2**), 2,4,6-*tris*-(3,5-*di-methylphenoxy*)-1,3,5-*triazine* (**3**) and 2,4,6-*tris*-(4-*methylphenoxy*)-1,3,5-*triazine* (**4**) (Scheme 2). Such a series of homologous hosts with a more or less homologous series of possible guest compounds allows for the systematic investigation of the packing modes of **1**–**4**. The central triazine rings should provide the proper alternating polarization needed for the Piedfort pair formation. The variation in the size and in the position of the substituents and in the applied solvents serve the means of exploring the prerequisites of inclusion formation *via* the Piedfort manner.

EXPERIMENTAL RESULTS

Compounds **1**–**4** have been synthesized from trichloro-*s*-triazine (cyanuric chloride) and the respective phenols following a literature procedure [10]. Presumed hosts **1**–**4** were dissolved in a variety of solvents. The range of putative guests comprised protic and aprotic, aromatic and aliphatic, low and high permittivity solvents (Tab. I). Since compounds **1**–**4** possess slightly basic *N* atoms in the triazine rings the choice has fallen first on a homologous series of simple aliphatic carboxylic acids. Formic acid, acetic acid and propionic acid were all acceptable solvents to a somewhat varying degree, also depending on the host molecule. However, solubility with the higher homologues decreased drastically. Series of 6-membered cyclic compounds both of aliphatic (cyclohexane, cyclohexanol, 1,4-dioxane) and of aromatic nature (benzene, toluene, *p*-xylene, pyridine) as well as some 5-membered carbocycles or heterocycles and higher alcohols were also probed to grow crystals.

TABLE I Crystalline inclusion compounds of **1**[a]

Guest solvent[b]	Stoichiometric ratio (1: guest)
Cyclopentane	1 : 2
Cyclopentene	1 : 1
Cyclohexane	2 : 3[c]
Cyclohexene	2 : 3
Benzene	2 : 3[c]
Tetrahydrofuran	1 : 2
1,3-Dioxolane	2 : 1
1,4-Dioxane	2 : 1[c]
Acetone	2 : 1
Nitromethane	3 : 1
Ethyl acetate	2 : 1[c]
Acetic acid	1 : 1[c] (**1a**)

[a] See Experimental section for methods of preparation, drying standard and characterization.
[b] Methylcyclohexane, *n*-hexane, *n*-heptane, toluene, *o*-, *m*-, *p*-xylene, mesitylene, pyridine, DMF, DMSO, cyclopentanone, triethylamine, ethanol, 1-propanol, 2-butanol, *t*-butanol, cyclopentanol, cyclohexanol, formic acid, propionic acid which were also tested as guest solvents, yielded no inclusion compounds.
[c] Stoichiometric ratios determined from X-ray structures.

The first crystallizations of **1** from simple aliphatic acids led to the observation of dimorphism. On crystallizing **1** from formic acid the so called α-form yields while from propionic acid the other β-form appears. With acetic acid, however, **1** forms a 1 : 1 inclusion compound (**1a**; Tab. I). The unit cell parameters of the crystals obtained from *p*-xylene, pyridine, *n*-hexane and cyclohexanol agreed within experimental error with that of the α-form. However, **1** yielded Piedfort type inclusions also from the low permittivity solvents 1,4-dioxane, cyclohexane, ethyl acetate and benzene [11].

The molecular structure of **1** shows a considerable variability in the above three crystal structures (α-**1**, β-**1**, **1a**). The differences between the observed conformers may best be expressed in terms of two torsion angles. The Cl—O—C_i—$N_{i\pm1}$ torsion angle is *peri*planar (*syn*- or *anti*-) in all the structures we report and in other triazine-trieters as well [6, 12]. This observation is attributed to the conjugation of the lone pair on the O atom with the ring π electrons [12a]. As to the variation of these torsions being *syn* or *anti*, there are four basic possibilities which these three substituents may adopt. Either there are all *anti* or *syn* values, or there are one *syn* and two *anti* values and *vice*

versa. Changing the N-atom selection renders *anti* equal *syn*, thus the number of the possibilities reduces to two basically symmetric conformations. The full *anti* conformer is thus called type **I** in this paper and the one with one different (*syn*) torsion angle is defined as type **II** (Fig. 1). There is, nevertheless, a further parameter to aid molecular shape description. This is the inclination angle of the phenoxy moieties, expressed by the C2—C1—O—C torsion angle here (defined as τ hereinafter). It renders further distinction between the conformers (Fig. 1c). If τ is greater than 90° we designate it by a slash "/" character, if τ is less than 90° then a backslash "\" is used as a shorthand for the aromatic ring inclination towards the central ring. The notation imitates the side view of the phenyl ring when looking at the molecule from the direction of the phenoxy substituent.

Accordingly (Tab. II), the molecular structure in the α-crystal form of **1** has the type **II** conformation (Fig. 2). All bond lengths agree with

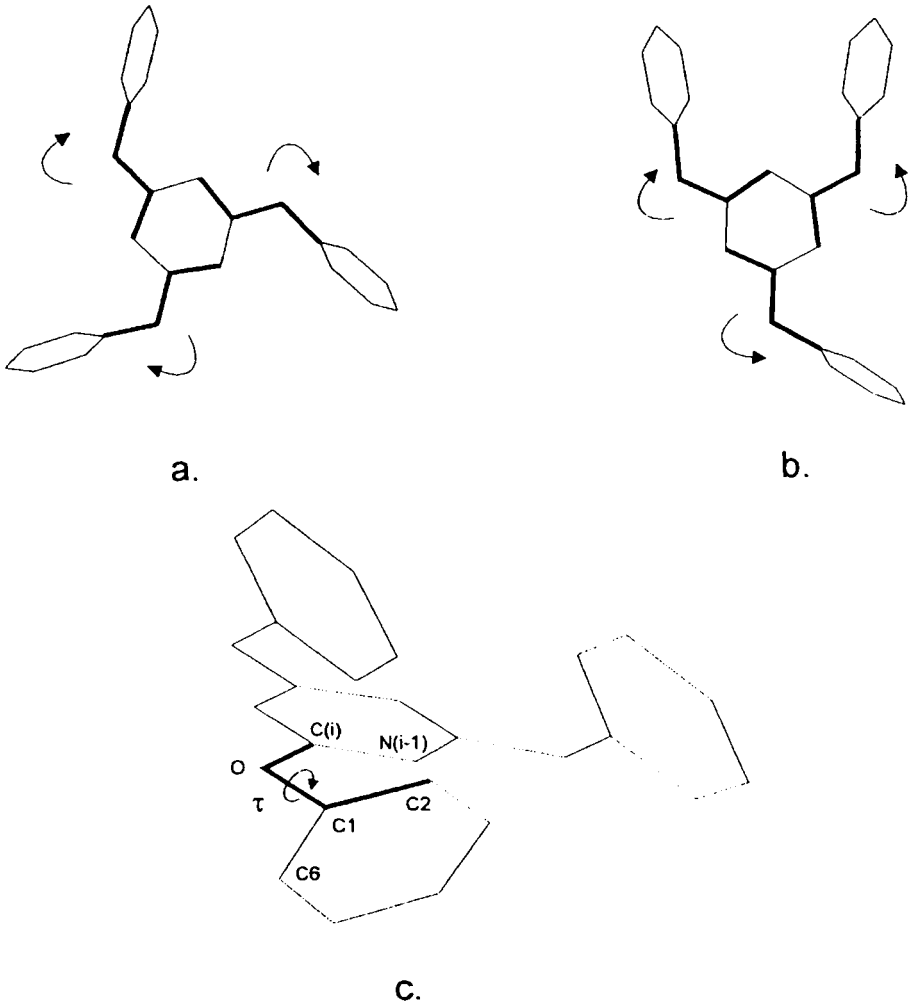

FIGURE 1 Definition of the conformational parameters. All three C1 O—C_i—N_{i-1} torsion angles are *anti-peri*planar in type I conformers (a), while one of them is *syn-peri*planar in type II conformers (b). Definition of the τ torsion angle is shown in (c). C2 and C6 are equivalent because of the symmetry of the substituent. Thus one can select either to get positive value of the torsion angle.

TABLE II Conformational descriptors of the molecular shapes in the crystals of the host molecule 1 and in the molecules 3 and 4 as well

	α-1		β-1		1a	3	4
Type	II		II		I	I	I
Tors. angle τ_1	94		88		82	79	89	70
Tors. angle τ_2	69		65		76	98	89	70
Tors. angle τ_3	65		65		73	86	89	70

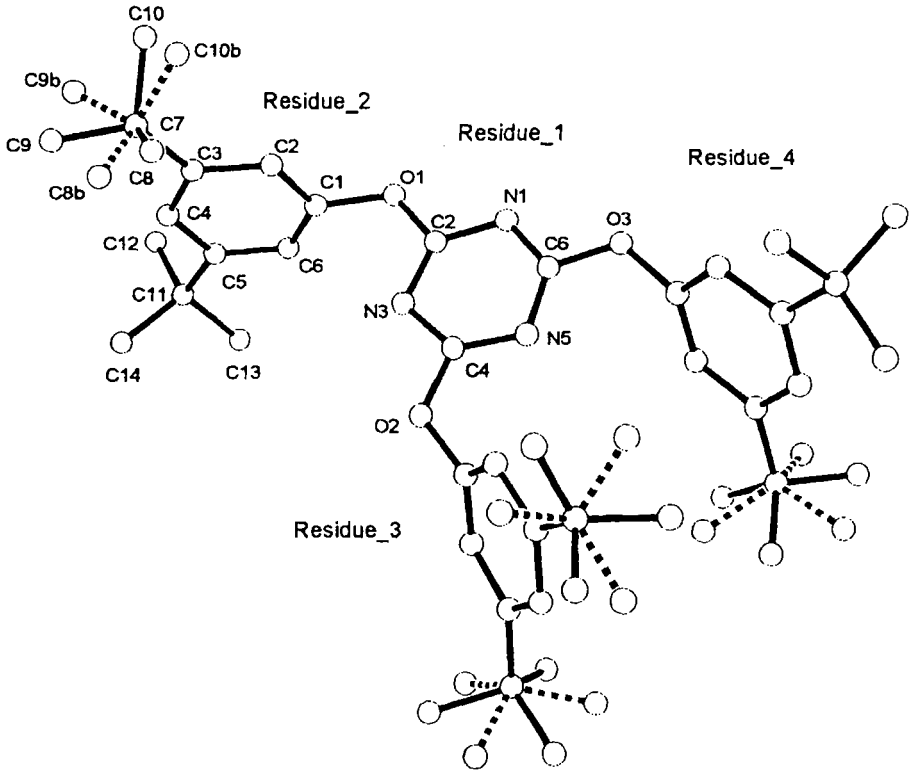

FIGURE 2 Molecular structure of 1 in the α-form. Secondary components of the disordered *t*-butyl groups are drawn with dashed bonds. Hydrogen atoms and thermal ellipsoids are omitted for clarity. See the Experimental section for details. Residues 3 and 4 are numbered the same way as residue 2.

the expected values and atomic displacement parameters are also normal except for atoms of the disordered *t*-butyl groups. The planes of the two phenyl rings close to each other are nearly parallel possibly because of steric reasons. The third ring is, however, tilted in the other way. Thus the simplified notation to describe this conformation is **II**-(\ //).

There are two molecules in the asymmetric unit in the crystal of the β-form (Fig. 3). The geometry of both molecules corresponds to expectations except for the disordered *t*-butyl groups. Both molecules have type **II** conformation. Contrasting the α-form, however, all three phenyl rings, two close to each other and the third distant one, incline in the same direction from $\tau = 90°$ thus forming a type **II**-(\\\) shape. The difference in the torsion angles τ of the two molecules in the asymmetric unit (Tab. II) also excludes a pseudo-symmetry operator between the two entities.

The host molecule in **1a** (**1**·acetic acid) adopts the all-alike type **I** conformation (Fig. 4). Appar-

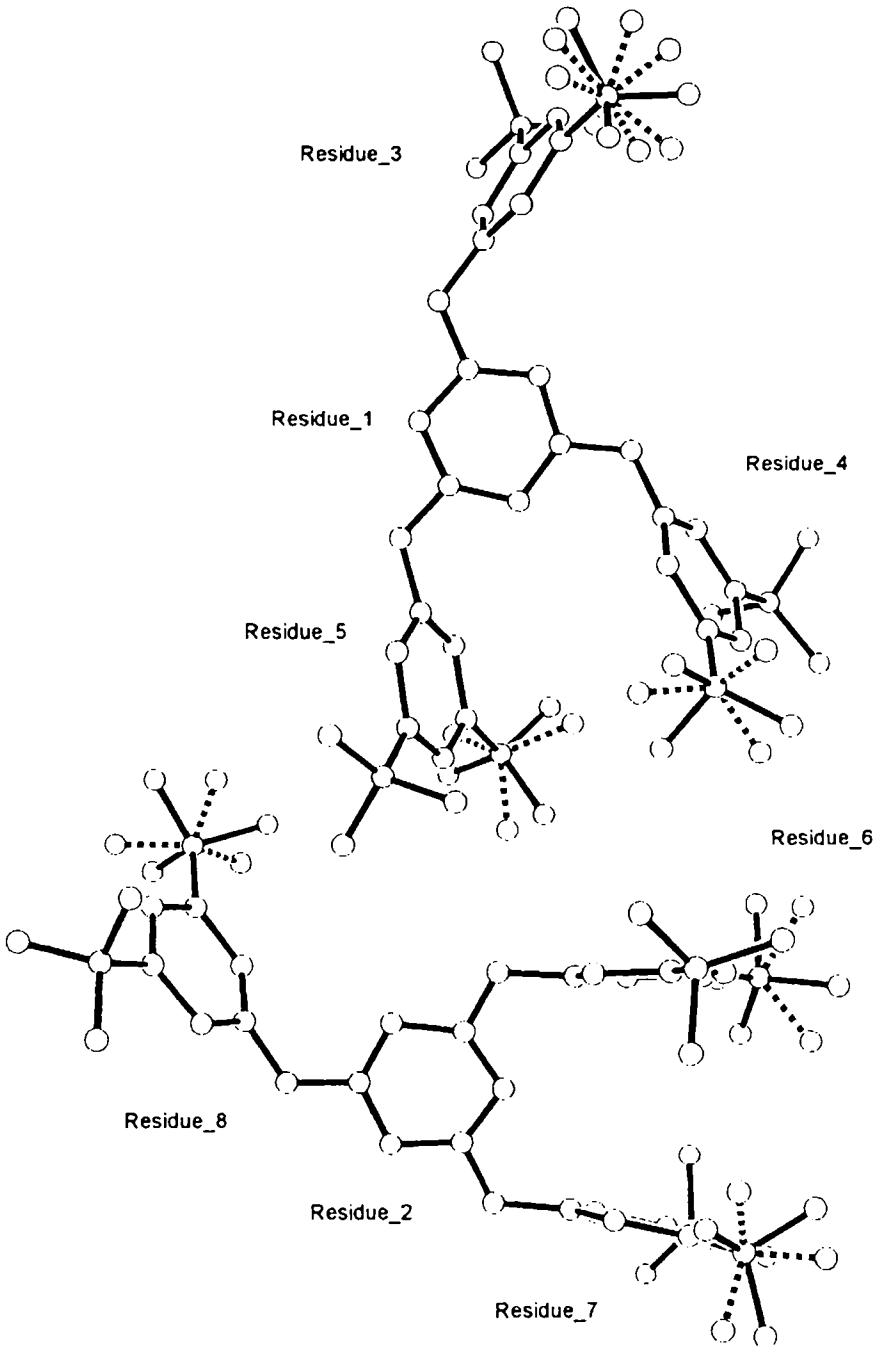

FIGURE 3 Structure of the two molecules in the asymmetric unit of the β-**1** crystals. Bonds to the secondary components of the disordered *t*-butyl groups are drawn with dashed lines. Hydrogen atoms and thermal ellipsoids are omitted for clarity. Atom numbering is the same as shown in Figure 2.

ently there are no steric restrictions in type I conformers as to the τ angle of the three substituent residues. Conformation of type I-(/\\) is observed in the inclusion crystal. The bond lengths and angles of the host molecule are similar to those in the dimorph crystals. The

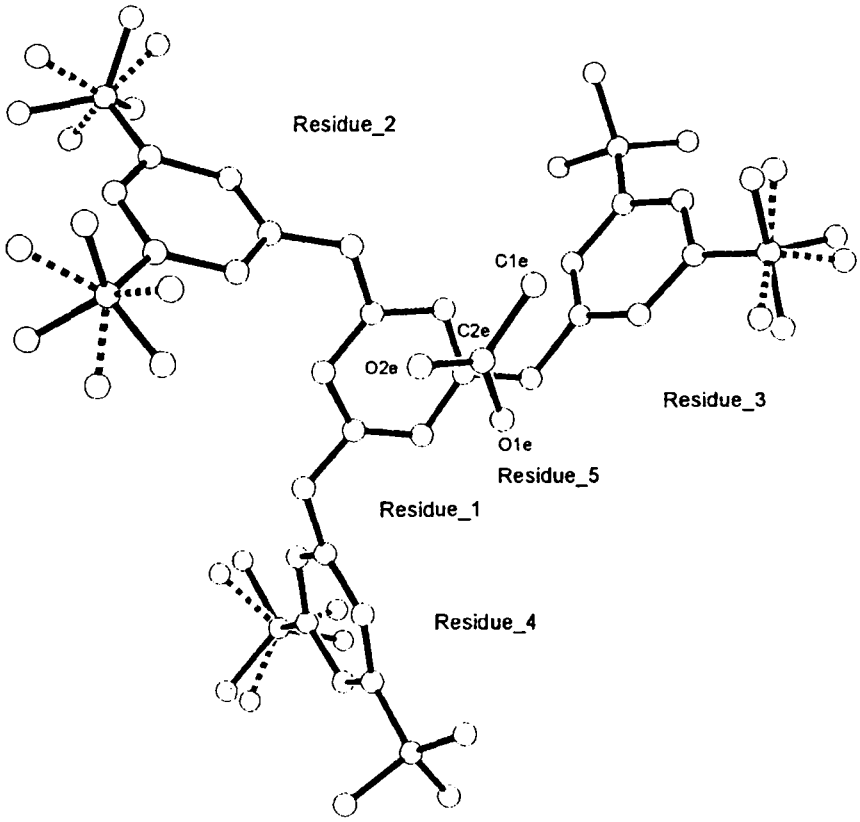

FIGURE 4 The asymmetric unit of **1a** contains one host and one guest molecule. Secondary components of the disordered *t*-butyl groups are drawn with dashed bonds. Hydrogen atoms and thermal ellipsoids are omitted for clarity. The atom numbering of the host molecule is the same as in Figure 2, only the numbering of the guest molecule (residue 5) is indicated.

t-butyl groups are disordered here as well. The C—O bond lengths of the guest molecule are of intermediate values (1.248 Å and 1.282 Å) indicating probable positional disorder around a proximal inversion center.

Both dimorphs crystallize in the same $P2_1/c$ (Nr. 14) space group. (The structure of the β-form was solved in the $P2_1/n$ setting.) The crystal packing of the two forms is illustrated in Figures 5 and 6, for the α- and β-forms, respectively. Fairly large voids were found in the crystal structure of the α-form. However, no substantial residual electron density could be located in these cavities. Preliminary thermogravimetric measurements also suggest that they do not contain solvent molecules [13].

There are no strong specific intermolecular interactions in these crystals. It is also apparent from these figures, that neither form of the dimorphic **1** molecules exhibit Piedfort-pairing behavior in their pure host forms. This is an interesting contrast to the first reported *sym*-1,3,5-triazines, where Piedfort formation does occur in the pure host crystal [6].

Nevertheless, the host molecules **1** do form Piedfort units in the inclusion crystals **1a** (Fig. 7). Acetic acid guest molecules form a dimer in a cavity between two pairs of Piedfort units. The two molecules of the host unit as well as the two acetic acid molecules are related by two independent centers of inversion. This represents a simple way of installing Piedfort-type inclusions. The basic building block with a centrosymmetric guest-dimer between two Piedfort units is repeated by unit cell translations. As it appears from this structure and other related

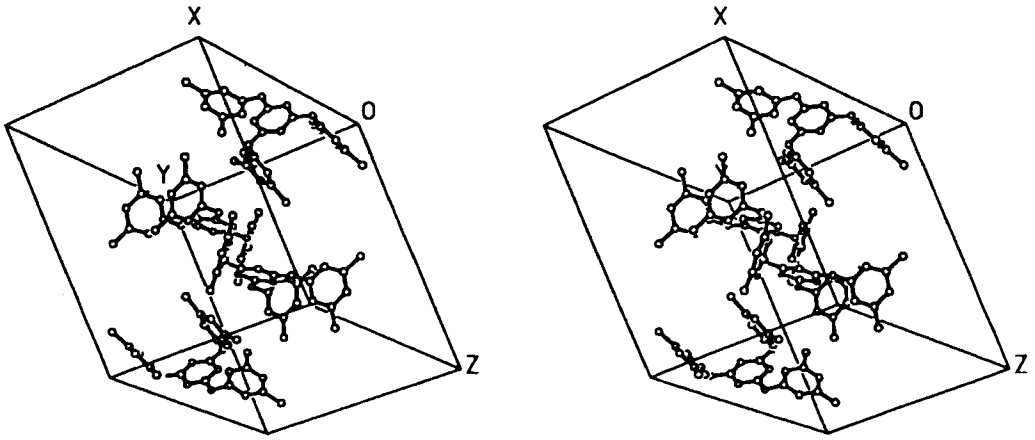

FIGURE 5 Crystal packing of the α-dimorph of **1**. Hydrogen atoms are removed and *t*-butyl groups are indicated as one atom for clarity.

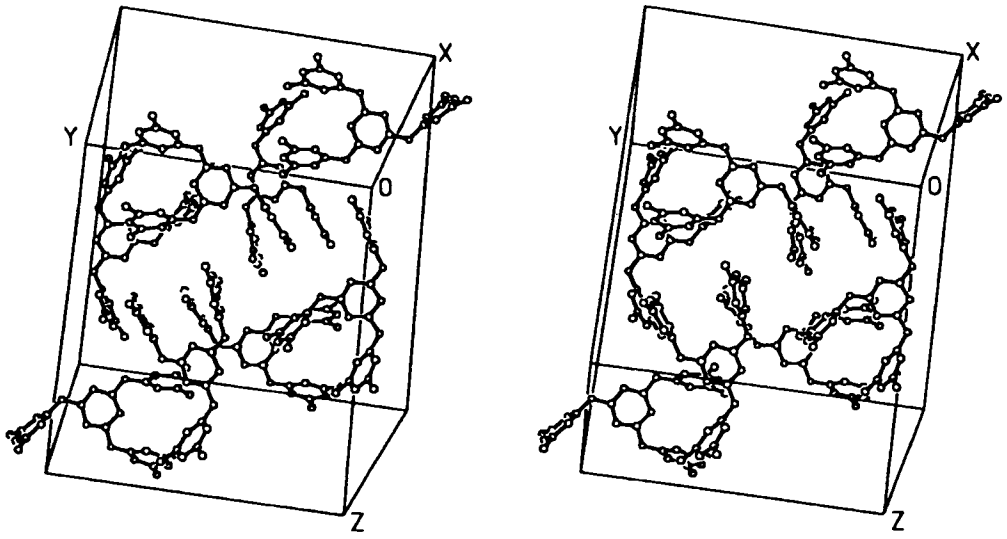

FIGURE 6 Crystal packing of the β-dimorph of **1**. Hydrogen atoms are removed and *t*-butyl groups are indicated by one *t* —C atom for clarity.

ones, formation of a Piedfort-unit may well be a solvent-driven phenomenon.

The crystals of a probable clathrate of **2** grown from dioxane were extremely labile and decomposed on removing from the solution within a few minutes. Up to now we were unable to grow suitable single crystals of this compound. The fast decomposition, however, suggests that an inclusion compound was formed as these crystals are usually less stable.

Compound **3** did not form inclusion compounds with the investigated range of solvents (*cf.* Tab. I). The cell parameters of the crystals obtained from these solvents (*e.g.*, 1,4-dioxane, 1,2-dichloroethane, dichloromethane, tetrahydrofuran and pyridine) were all the same. Recently, an independent X-ray study of **3** reported [4b] a structure identical with that of the crystals obtained by us from 1,4-dioxane. Thus we discuss structure **3** only to the extent

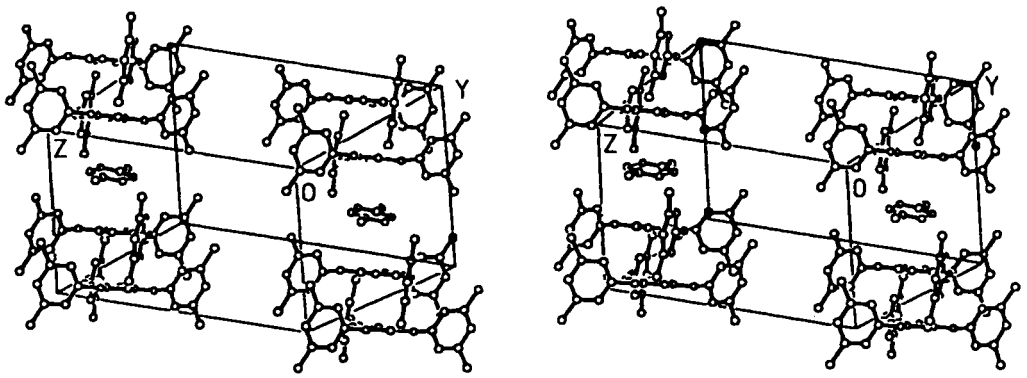

FIGURE 7 Crystal structure of the associate crystals of **1** with acetic acid dimers. Hydrogen atoms are removed and *t*-butyl groups are shown by one *t* —C atom for clarity.

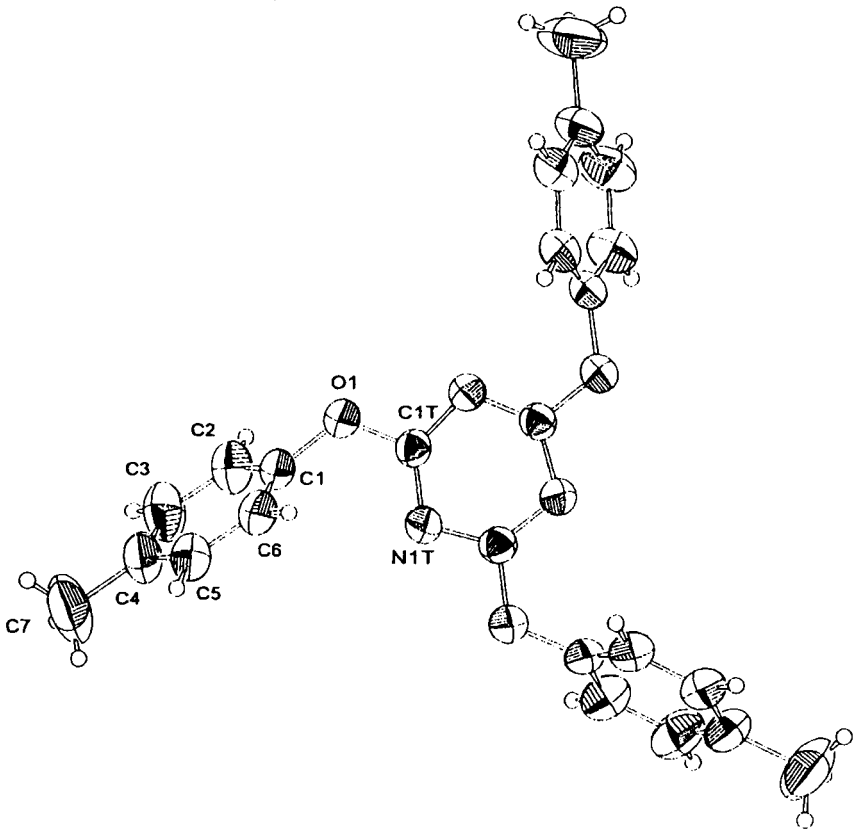

FIGURE 8 Molecular structure of **4**. Anisotropic displacement parameters are at the 50% probability level and H atoms are shown as spheres of arbitrary radius. The asymmetric unit contains only one third of the molecule (the numbered atoms).

required by this work and not necessarily emphasized in Thalladi *et al.* [4b].

We could only grow single crystals of **4** from *n*-hexane. These crystal structures indicate for both **3** and **4** that no solvent molecule incorporation occurred.

The molecules of **4**, like that of **3**, [4b] adopt perfect threefold symmetry with standard bond

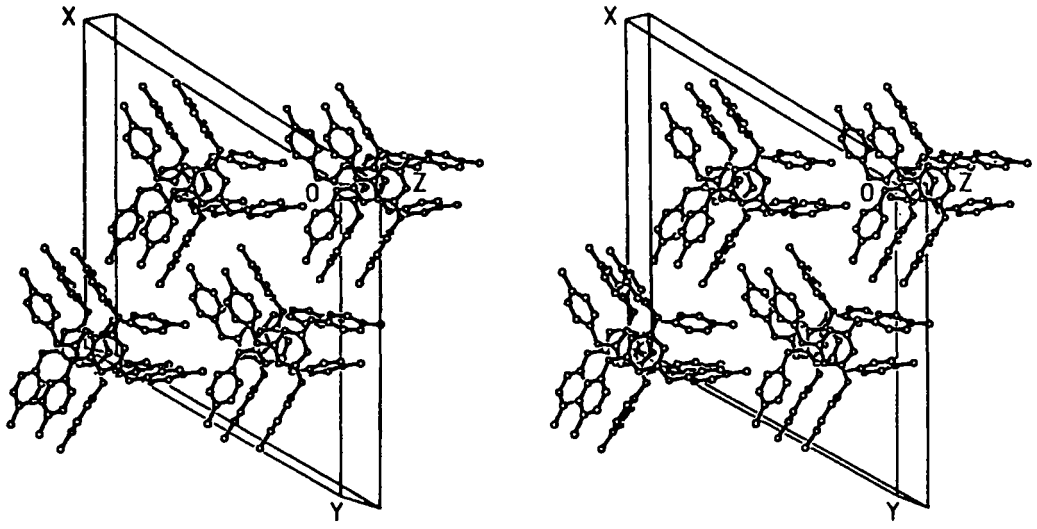

FIGURE 9 Crystal structure of **4**. A view from the *ab* plane shows the symmetry related molecular stacks in the rhombohedral unit cell. The vertical offset of these stacks is determined by the rhombohedral centering (see Scheme 3).

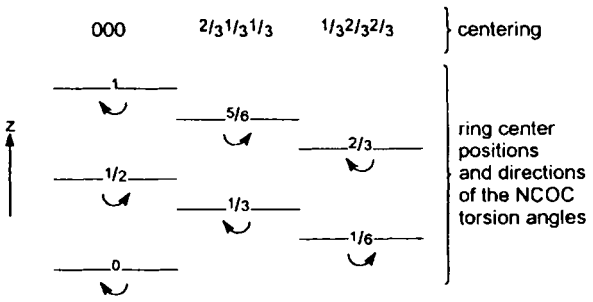

SCHEME 3

lengths and angles and with relatively large displacement parameters of the methyl groups (Fig. 8). Accordingly, **4** is of conformation type I-(\\\). The molecules of **4** thread and stack along crystallographic threefold rotors, which coincide with the molecular symmetry axes. The molecules in a stack are propagated in the unit cell by a *c* glide plane at $(2x, x, z)$. While the crystals of **3** are built from the parallel stacks *via* simple translations and there is no offset between the adjacent stacks, they are translated relative to each other by 1/6 along *c* in **4** corresponding to the rhombohedral centering (Fig. 9, Scheme 3). This out-of-plane offset is attributable to the increased space demand at the *para* position due to the *p*-methyl substitution *vs.* the *m,m*-dimethyl substitution in **3**. The distance between the threefold symmetry axes comprising the neighboring polymeric stacks is 13.30 Å in **3** while it is 13.65 Å in **4**. The 0.35 Å increase is also a demonstration of the strain relief due to the *p*-alkyl groups.

COMPUTATIONAL RESULTS

The observed polymorphy phenomena of **1** suggested analysis of its conformational space using computational methods [14]. We searched for local energy minima using molecular mechanics geometry optimization from different chemically reasonable starting points. Four different energy minima were located (Tab. III).

TABLE III Molecular mechanics energies of the conformers of host molecule (**1**), as calculated for isolated molecules *in vacuo* using the cff 91 force field as implemented in Insight II [14]

Conformation	Energy [kcal mol^{-1}]
I-(///)	−165.92
I-(\//)	−165.85
II-(///)	−171.44
II-(/\\)	−171.40

Subsequently conformational energy profiles of the C1—O—C_i—N_{i-1} and of the C2—C1—O—C torsion angles have been calculated (Figs. 10 and 11).

From these computations it appears that the C1—O—C_i—N_{i-1} torsion angles have well-separated minimum energy positions either close to 0° (*sp*) or close to 180° (*ap*). The peak at

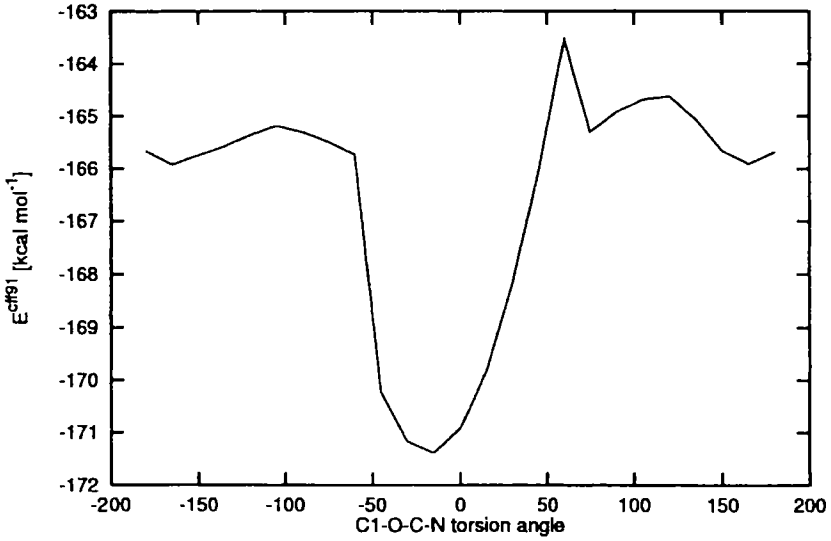

FIGURE 10 Conformational energy profile of the C1—O—C—N rotation in **1**.

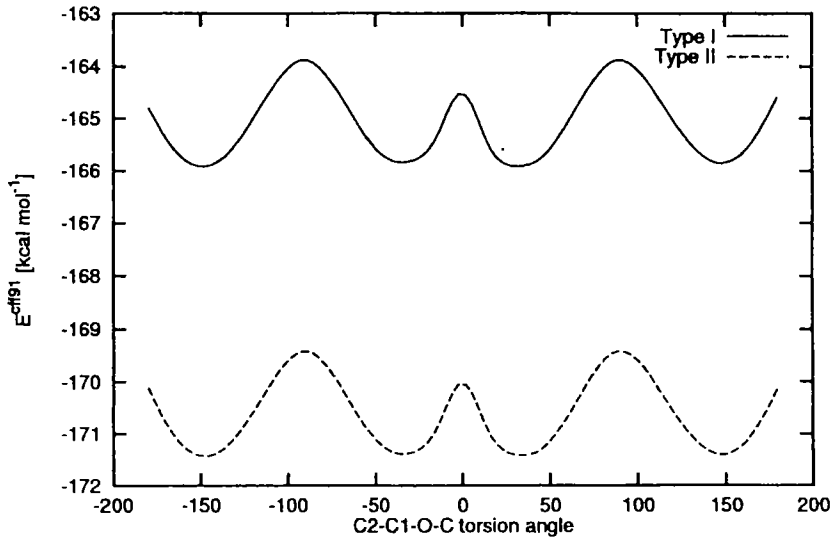

FIGURE 11 Conformational energy profile of the C2—C1—O—C torsion angle in **1**. The two graphs present the results for a type I conformer and for the independent ring of a type II one.

60° in Figure 10 is a consequence of impeding by a neighboring substituent. Note, that the plot is not symmetric because of this interaction with the rest of the non-symmetric molecule.

There are only two energy minima according to the changes of the C2—C1—O—C torsion angle, which correspond to 34° and 147° (*i.e.*, approximately +/−34°). The energy barrier between these two minima at 90° is about 2 kcal mol^{-1}. The symmetry of the plots in Figure 11 reflects the symmetry of the 3,5-di-*t*-butylphenoxy fragment. Thus, these results confirm the classification of the conformers as reflected by the solid state molecular shapes.

Further analysis shows that type **II** conformers are preferred energetically by approximately 5 kcal mol^{-1} (Tab. III). An inspection of the individual molecular mechanics terms reveals that this difference is attributable to the stronger nonbond dispersion in this conformation. The favorable interaction comes from the contact of the two di-*t*-butylphenoxy substituents. The energy difference between conformers of the same type is negligible.

Bearing in mind the peculiar crystallization behavior of **1** when exposed to formic-, acetic- or propionic acids we tried to account for the difference in the solvation of the different conformers in formic acid and in propionic acid. The intermolecular interaction energies of a solute with one to three acid molecules were calculated. However, simple molecular mechanics calculations did not show clear tendencies at all. Thus a more extended and environment handling treatment is deemed necessary. Considering the low barriers between the conformers, the role of nucleation and/or crystal growth processes may be decisive.

DISCUSSION

Conformation

Only *propeller shaped* host molecules can form Piedfort units and enclathrate guest molecules. Type **II** conformers observed only in the dimorphs of **1** are not analogous with the symmetry needed for hexahost-mimicry. One of the reasons for the different conformation of **1** is its bulkiness. The triazine rings cannot stack effectively because of the bulky *t*-butyl substituent. If a guest molecule fills the void between the adjacent pairs of molecules then **1** adopts type **I** conformation similarly to **3** and **4**.

Comparison of the Polymorphs

Crystallographically, the fundamental difference between the two modifications is the presence of one and two molecules in the asymmetric unit. This is one of the *a posteriori* explanations of the formation of the β-form.

The packing coefficient of the α-form has the rather low value of 0.52 in accord with the voids it contains. The cavities are surrounded by *t*-butyl groups. The calculated electrostatic potential of the molecule shows that there is a negative region around the aromatic groups while positive potential is observed around the *t*-butyls. Thus the existence of unoccupied regions in the α-form is explained both by the electrostatic repulsion of its surroundings and by the poor shape complementarity of the bulky *t*-butyl groups.

The two molecules within the unit cell of the β-form complement each other better so the molecules can pack more effectively (Fig. 6). As more favorable interactions are present in the β-structure the packing coefficient increases to 0.61. Thus, on the basis of the packing one may anticipate the β-form to be more stable than the α-one. As Gavezzotti alluded to, higher density often means higher packing energy though there is not a true correlation [15].

Inclusion Formation

The only efficient host molecule is **1**. The reason for this is its specific bulkiness, *i.e.*, it has a large enough bulk at the proper position. When this

condition is met two host molecules, while forming a Piedfort unit, can not have a third one stacked on them due to these massive substituents. As the *t*-butyl groups hinder the effective stacking of the host they also provide the void for inclusion. The effect of these steric conflicts is demonstrated by the large spacing between the stacked Piedfort pairs. The mean planes distance is 7.10(3) Å between two triazine rings encircling the guest molecules in **1a**. One may also speculate that the instability of the crystals of **2** can be attributed to the weaker repelling effect of the only substituent in *para* position. In a molecule of type **I** conformation the steric congestion exerted by the *para* position is approximately perpendicular to the direction of stacking, while in *meta* positions it is inclined to act parallel to the stacking direction. Accordingly, *m*-substituents must repel more than *p*-substituents.

As steric hindrance reduces due to the smaller alkyl size, the Piedfort pairs of the methyl substituted compounds **3** and **4** can stack effectively and form crystals without intervening guest molecules. (The packing coefficients of 0.64 for both **3** and **4** indicate the tightest packing in this series.) As a combined result of diminished repulsion and effective use of the threefold crystallographic rotors, *interstack* spans, *i.e.*, the distances between Piedfort pairs reduce from 7.10 Å to virtually the same value as the Piedfort base stacking values themselves (Tab. IV). Thus *polymeric* homomolecular stacks of Piedfort pairs assemble instead of inclusion formation. These stacks thread on threefold axes yielding to columns.

The distances between the mean planes of stacked Piedfort stacks of triazine rings decrease gradually from the value in the crystal structure of the *m*-dimethyl substituted **3**, through the *m*-monomethyl substituted equivalent [4b] until its smallest value in the *p*-methyl substituted **4** (Tab. IV). Thus, the *meta*-disubstituted methyl analogue **3** is somewhat closer to being a host than **4** is.

TABLE IV Intra- and inter-associate distances between the mean planes of triazine rings in the stacked molecules of Piedfort-pairs in **1a** and in the polymeric Piedfort stacks of **3**, **4** and 2,4,6-tris(3-methylphenoxy)-1,3,5-triazine (**5**) [4b]

Compound	Distance
1a	3.42(3) Å[a]
3	3.97(2) Å[b,c]
	4.01(2) Å[b,d]
4	3.332(1) Å
5	3.627 Å[c]
	3.569 Å[d]

[a] Distance between the molecules of a Piedfort unit.
[b] Respective data from Thalladi *et al.* [4b] are 3.970 and 4.029 Å.
[c] Inter-associate distance between molecules related by twofold axis.
[d] Distance between molecules related by inversion center.

One may thus conclude that *para* alkyl substituents are weaker repulsors in the stacking direction that one *meta* substituent and much weaker than two of the same substituents in *meta* positions. The direction of methyl groups in Figure 9 is instructive in this respect. This substitutional sequence bears practical importance for crystal engineering purposes. It allows fine-tuning of the stacking distance in combination with solvent effects, host symmetry and threefold molecular stacking like Piedfort pair formation.

Whereas the crystals of *meta*-chloro and *meta*-methyl substituted 2,4,6-triaryloxy-1,3,5-triazines are isostructural, the *para*-methyl derivative (**4**) and its chloro-analogue are completely different [4b]. Clearly, the geometrical requirements of the favorable C1···C1 contact observed in the chloro compound are not fulfilled in **4**. C1 atoms are replaced and the unfavorable alky···alkyl repulsions yield to a differing crystal packing.

CONCLUSION

The results of this study into some Piedfort host candidates based on symmetrically trisubstituted triazine rings provided general consequences as to the realization of such a design strategy. Since this kind of supramolecular systems is constructed by a multitude of supramolecular effects, the conclusions emanating

from this study are somewhat qualitative in their nature. These can be summarized in the following points.

- The central aromatic 6-membered ring must be properly polarized resulting in an alternating +/− charge distribution. This may be simply the consequence of either *sym*-1,3,5-trisubstitution [6] or *sym*-1,3,5-heteroatom substitution or a combination of both.
- Since the interaction between the juxtaposed 6-membered rings in a Piedfort pair is of fairly weak cohesion, one may suppose that the rings must be properly shielded from other competing interactions by a minimum of bulk and by a minimal length of the substituent arms.
- The stacking of aromatic (triazine) rings is a favorable interaction. The proper shape of the bulk must hinder sterically too close approach of Piedfort pairs in order to avoid the formation of homomolecular stacks. In other words properly sized and placed bulk must maintain enough empty space around the Piedfort pairs allotted for putative guests.
- The right place in this sense means that the bulky substituents must protrude in the expected direction of stacking to keep Piedfort units away from each other to a proper measure. In case of these alkyl-substituted aromatic rings *meta* positions are preferred over *para* ones. It is to be expected that branched alkyl substituents are more suitable repulsors than their *n*-isomers since conformational flexibility of the latter type allows for variance in the direction of their protrusion.
- The role of the solvents is important. As it appears the formation of a Piedfort unit may well be a solvent-driven phenomenon as well. The analysis of the relationship between, *e.g.*, permittivity, Piedfort formation and inclusion formation in the applied range of solvents is somewhat inconclusive. As a general tendency one observes that Piedfort pair formation is preferred in the low permittivity solvents while high permittivity perhaps disprefers this kind of association. The anomalous behavior observed in the homologous series of the simple aliphatic acids in this study does not necessarily contradict to such a conclusion due to their different inclination to dimer formation.
- Formation of the novel polymeric Piedfort stacks, when embedding chirality in such host molecules must directly yield to crystals that have profitable NLO activities [4].

Obviously, a future design strategy should incorporate a systematic variation of the central aromatic ring. Earlier investigations appear to broaden the Piedfort concept into a more general design manner than used hitherto [16]. We expect that the modification of the substituent groups on the side arms can provide further exaggeration of the shielding and bulk properties. It may provide proper tools for inducing guest selectivity, too. This work complements results of the Desiraju group [4] providing further details on the crystal structures of symmetrically trisubstituted *s*-triazines and may promote the design of novel non-linear optical materials.

EXPERIMENTAL

Synthesis

2,4,6-*Tris*(*alkylphenoxy*)-1,3,5-*triazines* **1-4**. *General procedure.* A mixture of trichloro-*s*-triazine (cyanuric chloride) and of the respective phenol in a molar ratio 1:3-4 was stirred at 170–210°C for 5 h. After cooling to room temperature the solid reaction mixture was grinded and treated with boiling methanol. The residue was collected and recrystallized from pure or dilute acetic acid.

2,4,6-*Tris*(3,5-*di-t-butylphenoxy*)-1,3,5-*triazine* (**1**): 3,5-Di-*t*-butylphenol was used; white powder (42% yield), mp. 234–236°C; ^{1}H NMR (CCl_4) δ 1.25 (s, 54H, CH_3), 6.92 (s, 6H, o–ArH), 7.20 (s, 3H, p–ArH); IR (KBr) 1600,

1500 (C = C, C = N), 1485 (CH_3), 1390, 1360 (C —Me_3), Anal. Calcd for $C_{45}H_{63}N_3O_3$: C, 77.88; H, 9.15; N, 6.05. Found : C, 78.13; H, 9.25; N, 6.24.

2,4,6-*Tris*(4-*t-butylphenoxy*)-1,3,5-*triazine* (**2**): 4-*t*-Butylphenol was used; white powder (37%), mp 193–195°C (lit. [17] mp 192–193°C).

2,4,6-*Tris*(3, 5-*di-methylphenoxy*)-1, 3, 5-*triazine* (**3**): 3,5-Dimethylphenol was used; white powder (43%), mp 271°C (lit. [10] mp 268.5–269.5°C).

2,4,6-*Tris*(4-*methylphenoxy*)-1,3,5-*triazine* (**4**): 4-Methylphenol was used; white powder (54%), mp 215–216°C (lit. [17] mp 216°C).

Crystalline Inclusion Compounds

The inclusion compounds used for the stoichiometric analysis (Tab. I) were prepared by dissolving the host compound **1** under heating in a minimum amount of the respective guest solvent. After storage for 12 h at room temperature, the crystals that formed were collected, washed with diethyl ether or methanol, and dried (1 h, 15 Torr, room temp.). Host: guest stoichiometric ratios were determined by ^{1}H NMR integration.

Single Crystal Preparation

The appropriate solvent was added to 10–30 mg of each host candidate until it was completely dissolved under application of mild heat. The vial was covered to decrease the speed of evaporation. All the samples were kept at room temperature until single crystals of suitable size were grown.

X-ray Structure Determinations

Reflection data were collected on an Enraf-Nonius CAD4 diffractometer in the $\omega/2\theta$ scan mode. Data reduction was done by using the program XCAD4 [18]. Absorption was corrected for using ψ-scan data [19]. The non-hydrogen atoms were located using direct methods and Fourier techniques [20]. The positions of the hydrogen atoms were generated assuming standard geometry. Full matrix least squares refinements of F^2 led to convergence at the respective R values (Tab. V) [21]. The atomic positions in the disordered *t*-butyl regions are ill determined so we had to use constraints to obtain acceptable geometries. All heavy atoms were treated using anisotropic displacement parameters. The hydrogen atoms were refined using a riding model and their isotropic displacement parameters were also derived from that of the attached non-hydrogen atoms. Thermal ellipsoid plots were generated using Zortep [22] while other structure drawings by using PX [23].

Computational

All the molecular mechanics calculations were performed using the software Insight II and the force field cff 91 [14]. The energy minimizations were carried out using conjugate gradient algorithm until the maximum derivative was less than 0.1 kcal Å^{-1} and then the quasi-Newton-Raphson minimizer until the maximum derivative decreased below 0.001 kcal Å^{-1}. The torsion energy profiles presented are obtained using the following procedure: Starting from the I-(\\\\) energy minimum structure model the respective torsion angle was set to -180°. Then the model was minimized using a restraint potential to keep the above torsion angle fixed. The energies of the restrained minima are reported in Figures 12 and 13. Then the starting torsion angle was increased by 15° and the structure was minimized again. The procedure was repeated until the torsion angle reached 180°. The electrostatic potential of **1** was calculated using the semiempirical AM1 method as implemented in Insight II [14]. The geometry of the molecule was optimized starting from the α-1 structure prior to the electrostatic calculation.

TABLE V Summary of X-ray data for crystal structures of 1, 3 and 4

	α-1	β-1	1a	3	4
Empirical formula	$C_{45}H_{63}N_3O_3$	$C_{45}H_{63}N_3O_3$	$C_{47}H_{67}N_3O_5$	$C_{27}H_{27}N_3O_3$	$C_{24}H_{21}N_3O_3$
Formula weight	693.98	693.98	754.04	441.52	399.44
Crystal system	monoclinic	monoclinic	triclinic	hexagonal	trigonal
Space group	$P2_1/c$	$P2_1/n$	$P-1$	$P-3c1$	$R3c$
a[Å]	17.870(4)	17.759(4)	10.720(2)	13.295(2)	23.644(1)
b[Å]	16.064(3)	20.693(4)	16.083(3)	13.295(2)	23.644(1)
c[Å]	17.908(4)	23.856(5)	16.326(3)	15.946(1)	6.664(1)
α[°]	90.00	90.00	116.38(3)	90.00	90.00
β[°]	119.70(3)	101.13(3)	102.28(3)	90.00	90.00
γ[°]	90.00	90.00	98.74(3)	120.00	120.00
V[Å^3]	4465.4(16)	8601.9(31)	2364.3(8)	2440.9(4)	3226.3(5)
Z	4	8	2	4	6
ρ_{calcd}[g cm^{-3}]	1.032	1.072	1.059	1.201	1.234
μ[mm^{-1}]	0.494	0.513	0.534	0.079	0.670
F(000)	1512	3024	820	936	1260
Crystal color	colorless	colorless	colorless	colorless	colorless
Crystal size[mm]	0.35 × 0.25 × 0.15	0.70 × 0.60 × 0.50	0.25 × 0.20 × 0.13	0.40 × 0.30 × 0.30	0.40 × 0.25 × 0.25
T[K]	293(2)	293(2)	293(2)	293(2)	293(2)
Radiation	Cu-Kα	Cu-Kα	Cu-Kα	Mo-Kα	Cu-Kα
λ[Å]	1.54184	1.54184	1.54184	0.71073	1.54178
θ range [°]	2.85–66.42	2.85–75.59	3.19–65.90	2.55–26.51	3.74–74.80
Index ranges	$-21 \le h \le 18$; $0 \le k \le 19$; $0 \le l \le 21$	$-22 \le h \le 21$; $-25 \le k \le 0$; $-8 \le l \le 29$	$-12 \le h \le 0$; $-18 \le k \le 19$; $-18 \le l \le 19$	$-16 \le h \le 16$; $-14 \le k \le 14$; $-20 \le l \le 20$	$-29 \le h \le 14$; $-14 \le k \le 29$; $-8 \le l \le 7$
Reflns collected	8585	18752	9118	5168	4237
Independent reflns	7813	17849	8223	1696	1452
R_{int}	0.0121	0.0331	0.0114	0.0389	0.0300
Observed reflns[$I > 2\sigma(I)$]	4378	12010	4286	851	1356
Max/min transmn	0.9812/0.9369	0.9832/0.8668	0.970/0.755	0.9766/0.9690	0.879/0.522
Data/restraints/param	6048/72/579	15478/481/1135	6097/73/617	1696/0/104	1419/1/95
GOF on F^2	1.114	1.102	1.104	0.851	1.059
$R1/wR2[I > 2\sigma(I)]$	0.056/0.174	0.062/0.191	0.059/0.173	0.038/0.108	0.026/0.071
$R1/wR2$(all data)	0.129/0.213	0.098/0.221	0.143/0.221	0.110/0.125	0.029/0.074
Largest diff. peak/hole[eÅ^{-3}]	0.25/−0.19	0.61/−0.40	0.33/−0.15	0.11/−0.15	0.07/−0.08

Acknowledgments

We thank Mr. Csaba Kertész for collecting X-ray intensity data and Dr. János Madarász for the thermogravimetric analysis of α-1. This work was supported by the Hungarian Research Fund (OTKA grant No. TO 015811), Hungarian Academy of Sciences (AKP grant No. 96/2–671 2,4/24), the Deutsche Forschungsgemeinschaft (GRK 208) and the Fonds der Chemischen Industrie.

References

[1] (a) Vögtle, F. (1991). *Supramolecular Chemistry*, Wiley, Chichester; (b) Lehn, J.-M., *Supramolecular Chemistry*, VCH, Weinheim, 1995; (c) Atwood, J. L., Davies, J. E., MacNicol, D. D. and Vögtle, F. (Eds.), *Comprehensive Supramolecular Chemistry*, Pergamon, Oxford, 1996; (d) Desiraju, G. R. (Ed.), *The Crystal as Supramolecular Entity. Perspectives in Supramolecular Chemistry* 2, Wiley, Chichester, 1996.

[2] (a) Weber, E. (1987). *Top. Curr. Chem.*, **140**, 1–20; (b) Weber, E. (Ed.), *Supramolecular Chemistry I and II (Top. Curr. Chem.* Vols. 165 and 175), Springer-Verlag, Berlin-Heidelberg, 1993 and 1995.

[3] (a) Gavezzotti, A. (1994). *Acc. Chem. Res.*, **27**, 309–314; (b) Desiraju, G. R., *Crystal Engineering – The Design of Organic Solids*, Materials Science Monographs 54, Elsevier, Amsterdam, 1989; (c) Weber, E. (Ed.), *Design of Organic Solids* (Topics in Current Chemistry, 198), Springer-Verlag, Berlin-Heidelberg, 1998.

[4] (a) Anthony, A., Desiraju, G. R., Jetti, R. K. R., Kuduva, S. S., Madhavi, N. N. L., Nangia, A., Thaimattam, R. and Thalladi, V. R. (1998). *Crystal Engineering*, **1**, 1–18; (b) Thalladi, V. R., Brasselet, S., Weiss, H.-C. , Bläser, D., Katz, A. K., Carrell, H. L., Boese, R., Zyss, J., Nangia, A. and Desiraju, G. R. (1998). *J. Am. Chem. Soc.*, **120**, 2563–2577.

[5] (a) Moberg, C. (1998). *Angew. Chem. Int. Ed.*, **37**, 248–268, and references therein; (b) Stang, P. J. (1998). *Chem. Eur. J.*, **4**, 19–27, and references therein.

[6] Jessiman, A. S., MacNicol, D. D., Mallinson, P. R. and Vallance, I. (1990). *J. Chem. Soc., Chem. Commun.*, 1619–1621.

[7] MacNicol, D. D. and Wilson, D. R. (1976). *J. Chem. Soc., Chem. Commun.*, 494–495.
[8] Henderson, K., MacNicol, D. D., Mallinson, P. R. and Vallance, I. (1995). *Supramol. Chem.*, **5**, 301–304.
[9] Hunter, C. A. and Sanders, J. K. M. (1990). *J. Am. Chem. Soc.*, **112**, 5525–5534.
[10] Thruston, J. T., Dudley, J. R., Kaiser, D. W., Hechenbleikner, I., Schaefer, F. C. and Holm-Hansen, D. (1951). *J. Am. Chem. Soc.*, **73**, 2981–2983.
[11] The crystal structures and properties of the inclusion compounds between **1** and guests of non-acidic nature will be described in a forthcoming paper.
[12] (a) Glówka, M. L. and Iwanicka, I. (1989). *Acta Cryst.*, **C45**, 1765–1767; (b) Glówka, M. L. and Sobanska, A. W. (1994). *Acta Cryst.* **C50**, 1124–1126.
[13] Madarász, J., Personal communication. No weight loss was detected below 275°C (mp 236°C).
[14] Insight II User Guide, October 1995. San Diego, Biosym/MSI, 1995.
[15] Gavezzotti, A. and Filippini, G. (1995). *J. Am. Chem. Soc.*, **117**, 12299–12305.
[16] (a) Weber, E., Hecker, M., Koepp, E., Orlia, W., Czugler, M. and Csöregh, I. (1988). *J. Chem. Soc., Perkin Trans.*, **2**, 251–1257; (b) Czugler, M., Weber, E. and MacNicol, D. D., unpublished results.
[17] Grigat, E. and Puetter, R. (1964). Ger. Patent 1, 183, 507, [*Chem. Abstr.*, (1965). **62**, 14705].
[18] Harms, K., *XCAD4* Data Reduction Program for CAD4 Diffractometers, 1996.
[19] (a) North, A. C., Philips, D. C. and Mathews, F. (1968). *Acta Cryst.*, **A24**, 350–359; (b) Reibenspies, J., *DATCOR* Program for empirical absorption correction, Texas A and M University, College Station, TX, USA, 1989.
[20] Sheldrick, G. M., *SHELXS-86* Program for Crystal Structure Solution, Institut für Anorganische Chemie der Universität, Tammannstrasse 4, D-3400 Göttingen, Germany, 1986.
[21] Sheldrick, G. M., *SHELXL-93* Program for Crystal Structure Refinement, Institut für Anorganische Chemie der Universität, Tammannstrasse 4, D-3400 Göttingen, Germany, 1993.
[22] Zsolnay, L. and Pritzkow, H., *ZORTEP* An Interactive OR-TEP Program. University of Heidelberg, Germany, 1994.
[23] Párkányi, L., *PX 0.6c* A "kin" PLUTO program for creating crystal structure illustrations. Chemical Research Center, Budapest, Hungary, 1996.